PHILOSOPHICAL TRANSACTIONS OF THE ROYAL SOCIETY A MATHEMATICAL, PHYSICAL & ENGINEERING SCIENCES

The Influence of Human Activities on the Distribution of Hydroxyl Radicals in the Troposphere

R. G. Derwent

Phil. Trans. R. Soc. Lond. A 1996 **354**, 501-531
doi: 10.1098/rsta.1996.0018

The influence of human activities on the distribution of hydroxyl radicals in the troposphere

By R. G. Derwent

Atmospheric Processes Research Branch, Meteorological Office, London Road, Bracknell, Berkshire RG12 2SZ, UK

Contents

The free radical reactions occuring in the sunlit troposphere involving methane, carbon monoxide, oxides of nitrogen, ozone and water vapour, generate a distribution of hydroxyl radicals which play a major role in removing many of the trace gases emitted by human activities. The United Kingdom Meteorological Office two-dimensional (altitude and latitude) chemistry transport model is used to describe the trace gas life cycles and the fast photochemistry and hence to calculate the distribution of

Phil. Trans. R. Soc. Lond. A (1996) **354**, 501–531
Printed in Great Britain

hydroxyl radicals. The mean concentration of hydroxyl radicals estimated in the lowest 0–12 km of the atmosphere is 1.2×10^6 molecules cm^{-3} (0.74×10^6 molecules cm^{-3} over 0–24 km). This concentration is in good agreement with estimates based on the OH radical concentrations required to balance the budgets of methyl chloroform and ^{14}CO. The two-dimensional model was used to investigate the likely future methane concentrations that would build up in the Intergovernmental Panel on Climate Change IS92a emission scenario over the period up to the year 2050. Because of the decrease in likely future OH radical concentrations due to the influence of human activities, methane concentrations build up significantly faster than emissions. There are therefore important consequences for global warming from human interference in the oxidizing capacity of the troposphere.

1. Introduction

The atmospheric chemistry processes that occur in the troposphere play an important role in removing many of the trace gases emitted by the natural biosphere and many of the pollutants emitted by human activities. One removal route involves oxidation of trace gases by hydroxyl (OH) radicals to water soluble substances which are then subsequently incorporated into rain and snow. Hydroxyl radicals, which drive many of the tropospheric removal mechanisms, are produced by photochemical reactions driven by sunlight. Their importance arises from their high intrinsic reactivity with a wide range of trace gases and pollutants.

Reaction with tropospheric hydroxyl radicals accounts for the major removal processes of methane, carbon monoxide, organic compounds, halocarbons and the oxides of sulphur and nitrogen emitted by human activities. Weinstock (1969) estimated the tropospheric mean hydroxyl radical concentration from an understanding of the major role oxidation plays in the life cycle of carbon monoxide. His estimate of the global tropospheric mean hydroxyl concentration of 1.2×10^6 molecules cm^{-3}, which, although a slight overestimate, compares well with the value developed in this study (see table 1), over 20 years later.

The important and close coupling between the life cycles of methane, carbon monoxide, hydrogen, oxides of nitrogen and ozone in the troposphere was first pointed out by Levy (1971). The free radical species thought to be involved were hydroxyl OH, hydroperoxy HO_2 and methylperoxy CH_3O_2. The recognition of the importance of the atmospheric chemistry processes coupling these trace gas life cycles, changed our perception of the behaviour and fate of ozone in the troposphere. Until then the ozone life cycle had been considered to be controlled by stratospheric input and surface destruction. Crutzen (1974) pointed out that photochemical production and destruction of ozone dominated and were in approximate balance, with stratospheric input and surface destruction rather small, but of a similar magnitude.

In view of the importance attached to tropospheric oxidation, numerous attempts have been made over recent years to measure hydroxyl radical concentrations. Direct measurement of the concentrations of tropospheric hydroxyl radical concentrations has, however, proved exceedingly difficult. Presently, the only direct observations in the boundary layer are made by laser long path absorption spectroscopy over a 2.8 km pathlength at Julich, Germany (Kraft & Perner 1993). Although the current accuracy of 3×10^6 molecules cm^{-3} is adequate, global coverage is not a practical

PHILOSOPHICAL TRANSACTIONS OF THE ROYAL SOCIETY A MATHEMATICAL, PHYSICAL & ENGINEERING SCIENCES

Table 1. *Estimates of the mean concentration of hydroxyl radicals in the lower atmosphere*

reference	mean hydroxyl radical concentration (10^6 molecules cm^{-3})	notes
methyl chloroform method		
Lovelock (1977)	0.7	
Singh (1977*a*)	0.2–0.6	
Singh (1977*b*)	0.41	
Neely & Plonka (1978)	1.15	
Prinn *et al.* (1992)	0.81	ALE/GAGE network study
^{14}CO *method*		
Weinstock (1969)	1.2	
Volz *et al.* (1981)	0.65	0–15 km, pole-to-pole
chemistry-transport models		
Crutzen & Fishman (1977)	0.8	0–12 km, pole-to-pole
Derwent & Curtis (1977)	0.76	0–15 km, pole-to-pole
Chang *et al.* (1977)	1.68	
Wuebbles *et al.* (1994)	0.829	
this work	0.74	0–24 km, pole-to-pole
this work	1.01	0–12 km, pole-to-pole

proposition with this technique. Methods have therefore been devised to calculate or estimate globally averaged hydroxyl radical concentrations (Derwent 1988) and three such methods are used in this theoretical modelling study. They are described in the following paragraphs and include the methyl chloroform method, coupled chemistry-transport models and the ^{14}CO method.

Lovelock (1974) was the first to observe the presence of methyl chloroform in the troposphere, following its growing and widespread use as a solvent. Oxidation by tropospheric hydroxyl radicals was shown to be its major sink (Cox *et al.* 1976) and Lovelock (1977) pointed out that it could be used as an indicator of the tropospheric hydroxyl radical abundance. First estimates of the mean tropospheric hydroxyl radical concentration of about 7×10^5 molecules cm^{-3} were surprisingly accurate (see table 1). Since then refinements have been made to the methyl chloroform absolute calibrations (Butler *et al.* 1991), the global emission source strength (Midgley 1989) and the rate coefficent for the reaction of hydroxyl radicals with methyl chloroform (Talukdar *et al.* 1992). This is now considered a highly accurate method for determining the mean tropospheric hydroxyl radical concentration (Prinn *et al.* 1992).

There has been steady progress in improving our understanding of the life cycles of the major tropospheric trace gases and of the chemical kinetics of the photochemical and thermochemical processes which link them. Two-dimensional (altitude and latitude only) models have remained the main tools for evaluating the importance of candidate processes. They have been difficult to validate because of the dearth of atmospheric measurements of important species. Aircraft and ship-borne surveys,

as well as intensive field measurement campaigns, have dramatically extended our understanding of tropospheric composition. Progress is currently held up because of the difficulty of measuring NO_x concentrations in the unpolluted troposphere.

Nevertheless, coupled chemistry-transport models provide the second theoretical route to the estimation of the tropospheric distribution of hydroxyl radicals, in addition to the methyl chloroform route detailed above (Derwent & Curtis 1977; Chameides & Tan 1981; Brasseur *et al.* 1990; Taylor *et al.* 1991; Wuebbles *et al.* 1994). Early model estimates indicated a global tropospheric mean hydroxyl radical concentration of 7.6×10^5 molecules cm^{-3} (Derwent & Curtis 1977), which is in close agreement with the value reported in this study (see table 1). Many of the uncertainties in the chemical-transport model calculation method for tropospheric OH have been removed over the years by establishing databases of evaluated chemical kinetic data (Atkinson *et al.* 1992). The uncertainties which now remain are largely, but not wholly, concerned with global emissions source strengths.

A major uncertainty in the global tropospheric mean hydroxyl radical concentration derived from coupled chemistry-transport models is the emission source strength for carbon monoxide. Since the only constraints in the atmospheric budget and life cycle of carbon monoxide are the surface concentrations, model-derived tropospheric mean hydroxyl radical conentrations increase with the assumed magnitude of the carbon monoxide emission source strength. As originally pointed out by Weinstock (1969), an extra constraint can be introduced into the analysis by studying the isotopic distribution in carbon monoxide. Volz *et al.* (1981) used a coupled chemistry-transport model to determine both the source strengths of ^{12}CO and ^{14}CO and the tropospheric distribution of hydroxyl radicals. This third theoroetical method gave at that time a mean tropospheric OH concentration of 6.5×10^5 molecules cm^{-3} which is close to the value generated in this present study (see table 1).

The three basic methods (methyl chloroform, coupled transport-chemistry modelling and ^{14}CO) for the determination of the distribution of tropospheric hydroxyl radicals have been implemented in the two-dimensional (altitude latitude only) modelling study which is described below. The model used is constrained only by current understanding of the processes thought to be important in the trace gas life cycles and by their emissions. It is therefore possible to use this model, in addition, to assess the extent to which the tropospheric distribution of hydroxyl radical concentrations has been perturbed by human activities.

Human activities influence the tropospheric distribution of hydroxyl radicals through a range of possible mechanisms. First, each of the major tropospheric source gases: methane (Rasmussen & Khalil 1984; Blake & Rowland 1986), carbon monoxide (Cicerone 1988), oxides of nitrogen (Crutzen & Gidel 1983; Logan 1985) and hydrocarbons (Hough & Derwent 1990) has some emission sources which are either directly or partially influenced by human activities. Second, stratospheric ozone depletion leads to increased penetration of solar ultraviolet radiation into the troposphere below, which, all things being equal, would lead to increased tropospheric hydroxyl radical abundances (Thompson & Cicerone 1986). Third, climate change, driven by the increased radiative forcing of carbon dioxide, methane and ozone (Fishman *et al.* 1979) derived from human activities, will lead to higher global temperatures, shifts in relative humidities, cloud distributions and winds and hence may lead to changes in the sources and sinks of the major tropospheric trace gases.

In analysing the feasible environmental policy responses to the possible influences of human activities on the tropospheric distribution of hydroxyl radicals, it will be

PHILOSOPHICAL TRANSACTIONS OF THE ROYAL SOCIETY A MATHEMATICAL, PHYSICAL & ENGINEERING SCIENCES

necessary to evaluate a wide range of scenario assumptions concerning the future emissions of methane, carbon monoxide, oxides of nitrogen and hydrocarbons. It is important to determine whether future tropospheric hydroxyl radicals concentrations will be higher or lower than present day levels (Isaksen & Hov 1987). If future hydroxyl radicals concentrations are depressed then, all other things being equal, methane and halocarbon concentrations will rise above their current levels, increasing their global warming impacts.

2. Model description

(*a*) *Model structure*

An understanding of the behaviour of the tropospheric trace gases requires, in principle, a description in three dimensions of atmospheric dynamics, atmospheric chemistry and sources and sinks. The total problem is extremely complex and the computer requirements for any comprehensive scheme are enormous. In view of the requirements to make progress against this background with present limited understanding, simplifications are usually made along the following lines:

reducing the number of chemical species described,
reducing the dimensionality of the problem,
removing the meteorological equations,
limiting the spatial resolution,
averaging over time intervals.

The time-dependent behaviour of the tropospheric source gases, free radicals, temporary reservoir and oxidation products (see table 2), was represented in this study using the UK Meteorological Office zonally averaged two-dimensional model. The model is driven by the emissions, chemistry and wind fields appropriate to a model domain which extends from pole-to-pole and up to an altitude of 24 km. The model domain was divided up into $12 \times 24 = 288$ equal volume grid cells using 12×2 km vertical layers and 24 latitude bands, equally spaced in sine (latitude), with 12 in each hemisphere. The study period covered the time period of 1983 onwards. The model has the same conceptual framework as that used previously to show how oxides of nitrogen, carbon monoxide and methane emissions from human activities could well have caused a doubling in ozone concentrations close to the surface in the Northern Hemisphere since pre-industrial times (Hough & Derwent 1990).

The time dependence of the concentration, $[c_i]$, of species i, is represented by

$$\frac{\mathrm{d}[c_i]}{\mathrm{d}t} + \mathrm{div}([c_i]u) = S_i + \mathrm{div}(KN\,\mathrm{grad}([c_i]/N)), \tag{2.1}$$

where u represents the zonally averaged wind field, S_i the net source and sink term, K is an eddy diffusion tensor, and N is the atmospheric molecular number density. The net source and sink term comprises the chemical and photochemical production and destruction of the constituent, emission from the surface and deposition or other removal processes. In principle, all the various terms in equation (2.1) above have been described for an extensive range of trace gases so that the system of coupled equations can be solved with useful resolution for a range of practical policy problems.

(*b*) *Model transport*

The zonally averaged wind field, u, and eddy diffusion tensor, K, were taken from the work of Plumb & Mahlman (1987) who used the output from a general circulation

Table 2. *The model species*

tropospheric source gases		
water vapour	hydrogen	
nitrous oxide	nitric oxide	nitrogen dioxide
carbon monoxide	^{14}CO	
methane	ethane	propane
butanes	pentanes	hexanes
ethylene	propylene	acetylene
benzene	toluene	isoprene
terpenes		
methyl chloroform	$CHCl_2F$ (HCFC-22)	
reaction products		
ozone	nitric acid	
temporary reservoirs		
nitrogen pentoxide	pernitric acid	hydrogen peroxide
methyl hydrogen peroxide	ethyl hydrogen peroxide	
peroxyacetylnitrate	methylpernitrate	
formaldehyde	acetaldehyde	methylethylketone
glyoxal	methylglyoxal	methylvinylketone
methacrolein		
free radical species		
hydroxyl	hydroperoxy	nitrate
methylperoxy	ethylperoxy	butylperoxy
hexylperoxy	ethyleneperoxy	propyleneperoxy
arylperoxy	peroxyacetyl	acetoneperoxy
maleicdialdehydeperoxy	methylvinylketoneperoxy	methacroleinperoxy
steady state species		
O^1D	O^3P	H
CH_3		

model (Mahlman *et al.* 1980) to derive a mean meridional circulation and a tensor to describe the eddy motions present in the zonal flow. The values of the effective stream function and eddy diffusion coefficients were available on a grid of 75 equally spaced latitude points and nine unevenly spaced pressure levels for each month of the year. These data were processed on to the two-dimensional model grid. Full details of the inert tracer transport in this model using the Plumb & Mahlman (1987) circulation are given elsewhere (Hough 1989).

Following the work of Strand & Hov (1993), the vertical eddy diffusion coefficients provided by Plumb & Mahlman (1987) for the stratosphere have been reduced to the minimum value of $0.3\,m^2\,s^{-1}$. This change has an important influence on the ozone profiles in the lower stratosphere and brings them into closer agreement with observations, resolving some problems noted in earlier studies (Hough & Derwent 1990; Hough 1991).

The differential equations (2.1) for each species were then transformed on to an equal volume grid using

$$y = a \sin \theta,$$

where y is the horizontal coordinate in equation (2.1), θ is the latitude and a is the radius of the earth. These transformations are explained elsewhere (Curtis 1987*a*, *b*). The system of differential equations was assembled and integrated numerically using the Gear's method, automatic, stiffly stable computer progam FACSIMILE (Curtis & Sweetenham 1987). A 10 year integration of the $288 \times 54 = 15\,552$ simultaneous differential equations took about three days CPU time on a desktop work-station (DEC 3100).

The model is driven totally by the emissions, chemistry, transport, upper boundary conditions and deposition. There are no fixed concentration fields within the model domain or at the surface, other than for the atmospheric number density. There are also no redistributions of model concentrations to ensure that concentrations remain in agreement with observations, except for water vapour. The concentrations of all model species (table 2) were determined as variables of the model differential equations.

(*c*) *Emissions inventory*

Of the tropospheric source gases listed in table 2, 17 species are included in the model emissions inventory. This includes the most important species which are thought to play a part in driving global tropospheric chemistry. Table 3 provides a summary of the model assumptions with respect to emisions. The hydrocarbons represent surrogates for the many hydrocarbons emitted by both natural biogenic and by human activities. Each hydrocarbon also represents a weighted sum over all isomers.

Each of the source categories has been given a distinct distribution of its emissions with latitude and time of year. A brief description of the emission fluxes is given below and further details are available elsewhere (Hough & Derwent 1990; Hough 1991).

(i) *Methane*

The entries in table 3 for global methane emissions are based on the recent IPCC review (Houghton *et al.* 1992). A global methane source strength of 480 million tonnes per year has been used with natural wetlands, animals and human activities providing the largest contributions.

(ii) *Carbon monoxide*

The entries in table 3 for carbon monxide emissions are based on the literature review provided by Warneck (1988). Biomass burning and human activities (mainly the exhausts of petrol-engined motor vehicles) are the largest contributors. The entries, however, do not include the carbon monoxide derived within the chemical mechanism from the oxidation of methane, simple non-methane hydrocarbons and the natural biogenic hydrocarbons, which amount to 750, 110 and 645 million tonnes per year, respectively, in addition to the 1575 million tonnes per year in table 3.

(iii) *Oxides of nitrogen*

The principal source of the oxides of nitrogen is from human activity and the global source strength of 21 million tonnes as nitrogen per year reflects this (Logan

Table 3. *The model emission inventory, giving emission rates in million tonnes per year*

human activities[a]		*soils and fauna*	
nitrous oxide	4.8 (as N)	nitrous oxide	7.8 (as N)
NO_x	21.0 (as N)	NO_x	5.0 (as N)
carbon monoxide	650.0	hydrogen	5.0
hydrogen	20.0		
methane	155.0	*biomass burning*	
ethane	6.0	NO_x	8.00 (as N)
propane	6.0	hydrogen	20.00
butane	10.0	carbon monoxide	800.00
pentane	10.0	methane	40.00
hexane	15.5	ethane	0.95
ethylene	10.0	propane	1.25
propylene	10.0	ethylene	1.90
acetylene	2.5	propylene	1.60
benzene	5.0	nitrous oxide	0.70 (as N)
toluene	15.0		
vegetation		*other sources of methane*	
carbon monoxide	75.0	ruminants	105.0
ethane	15.0	natural wetlands	115.0
propane	15.0	paddy fields	60.0
butane	8.0	*other* NO_x *sources*	
pentane	6.0	lightning	8.0 (as N)
hexane	6.0		
ethylene	20.0		
propylene	20.0		
isoprene	450.0		
terpenes	550.0		

[a] Including combustion, motor vehicles, chemical processes, oil and gas production, etc.

1983; Crutzen & Gidel 1983; Dignon & Hameed 1989). The smaller sources include biomass burning (Logan 1983), soil exhalation (Ehhalt & Drummond 1988) and lightning fixation (Logan 1983; Chameides *et al.* 1987).

(*d*) *Chemical mechanism*

The two-dimensional model adopts a detailed chemical mechanism approach and describes the time-dependent behaviour of the 54 model species with 91 thermal reactions, 27 photochemical reactions and five night-time reactions. The chemical mechanism is explained in detail in Hough (1991). Rate coefficients for the thermal reactions are taken from the evaluated chemical kinetics database of Atkinson *et al.* (1992). Explicit treatment of the temperature and pressure dependences of all rate coefficients is included where information is available. One rate coefficient, that of the HO_2 self-reaction has a water vapour dependence which is also carefully represented. Temperature values were assembled for each model grid cell on a monthly basis from the data of Oort (1983) and Barnett & Corney (1985).

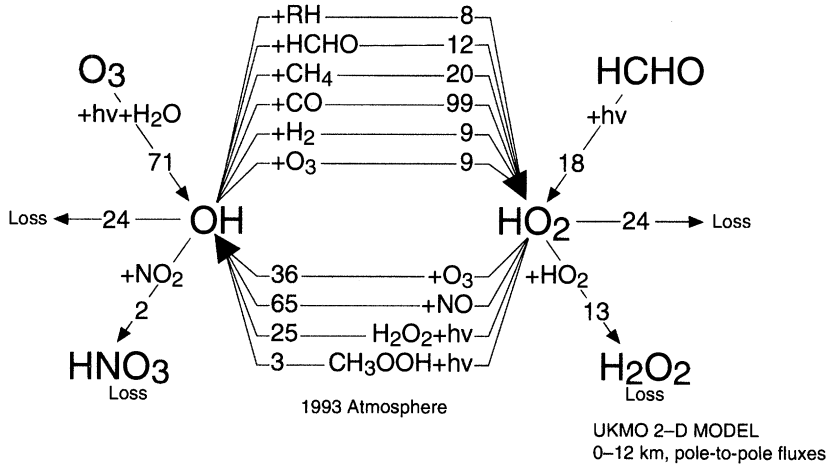

Figure 1. The fast photochemical balance in the troposphere, reaction fixtures in 10^{12} mol a^{-1}.

Photochemical rate coefficients were calculated from the overlap of the solar actinic flux with the absorption cross-section and quantum yields of the photochemically labile molecules, with wavelength over the range from 200–600 nm. Solar actinic fluxes were calculated from the solar irradiance at the top of the atmosphere (WMO 1986), taken to be 50 km, using a two-stream isotropic multiple scattering algorithm (Hough 1988). This algorithm dealt with absorption by molecular oxygen, stratospheric ozone, tropospheric aerosols, three cloud layers and surface albedo. Cloud amounts were predicted from model relative humidity using the method of Buriez *et al.* (1988) and compared with satellite data (Hughes & Henderson-Sellars 1985) and with a climatology (Warren *et al.* 1986). Absorption cross-sections and quantum yields were taken from the WMO review (WMO 1986).

The photolysis rates were calculated once each month as a diurnal average. First an average of the cosine of the zenith angle was estimated for each latitude band and each month for the daylight part of each day. From these, daytime average photolysis rates were calculated and multiplied by the fraction of daylight in each month to obtain daily average photolysis rates. A consequence of using daily average photolysis rates rather than following the full diurnal cycle in solar actinic fluxes, is that night-time chemistry is suppressed. Night-time and daytime NO_3 and N_2O_5 were treated as if they were separate species and this allowed their night-time build-up since they, and their precursors, were not then subject to photolysis. The night-time formation of N_2O_5, HNO_3 and precipitation nitrate could by these means be better represented.

Figure 1 lays out the processes incorporated in the chemical mechanism which are believed to form the main elements of the fast photochemical balance of the troposphere, based on the chemical reaction scheme of Hough (1991). In this figure, the mean annual reaction fluxes are presented through each elementary process averaged over 0–12 km, pole-to-pole. This balance system is active throughout the sunlit troposphere and accounts for the formation of a steady state concentration of hydroxyl radicals present at low concentration, 0.01–0.1 ppt or so. Despite this low steady state concentration, hydroxyl radicals are so highly reactive that they succeed in driving many of the tropospheric chemical processes. Figure 1 emphasizes roles of the free radical species OH and HO_2 and shows how they are interlinked by reactions

Table 4. *Removal processes in the two-dimensional model*

dry deposition			
	deposition velocity/(mm s^{-1})		
species	land	ocean	ice and snow
ozone	6	1	0.5
nitrogen dioxide	1	0.5	0.2
nitric acid	40	10	0.5
PAN	2	0	0
hydrogen peroxide	10	10	0.5
organic peroxides	5	5	0.5
hydrogen	0.45	0	0
carbon monoxide	0.3	0	0

wet deposition	
	Henry's law coefficient
	mol dm^{-1} atm^{-1} species
nitric acid	3.3×10^6
hydrogen peroxide	7.4×10^4
methyl hydrogen peroxide	2.2×10^2
formaldehyde	6.3×10^3
glyoxal	1.4×10^6
methyl glyoxal	3.7×10^3

with the tropospheric trace gases. The figure has been prepared by summing up the overall effect of many complex chemical reaction cycles within the chemical model. There is a slight overall out-of-balance in each of the OH and HO_2 gains and losses due to these simplifications. In the chemical model, the annual fluxes are necessarily exactly in balance.

(*e*) *Removal processes*

Chemical processes are not the sole determinands of the chemical development in the troposphere and account must be taken of the physical removal processes such as dry and wet deposition for certain species, particularly the temporary reservoir species (see table 4).

The dry deposition of the species in table 4 was represented for a range of underlying surface types. For such a species, the following term was added to the time rate of change of that species concentration:

$$\frac{\mathrm{d}[c_i]}{\mathrm{d}t} = \frac{vg_i}{h}[c_i],$$

where h is the depth of the lowest model layer, usually taken to be 2 km and vg_i is the species-dependent effective dry deposition velocity, in the grid cell concerned (see table 4).

Wet deposition was described for nitric acid, hydrogen peroxide, methyl hydrogen peroxide and the aldehydes using the model calculated local volume of liquid water

and temperature dependent values of the Henry's law coefficients for each species (see table 4).

(*f*) *Upper boundary conditions*

The upper boundary conditions for each model species were established at 24 km, in the lower stratosphere. For the majority of the model species, concentrations decrease with altitude and their exchange with the upper atmosphere is of negligible importance. However, for certain rather long-lived model species, chemical removal in the middle and upper stratosphere above the model domain cannot be ignored. An upwards flux out of the model domain was therefore included for those long-lived species by specifying their mixing ratio above the model as a fixed fraction of their mixing ratios in the model top layer. For ozone, a downwards flux into the model domain was described by prescibing an infinite reservoir of ozone above the model domain from SBUV/NIMBUS 7 satellite observations between 1978 and 1987 (Bhartia *et al.* 1984).

3. Results for some tropospheric trace gases

(*a*) *Methane*

The overwhelmingly dominant fate (98%) of the methane emitted at the model surface is reaction with hydroxyl radicals in the troposphere, with the remainder of the loss occurring in the stratosphere. Over the 10 year model calculation starting in 1983, though, sources and sinks for methane were not in accurate balance, with the former larger than the latter. As a consequence, methane slowly built up in the model troposphere with an average annual accumulation of 39 million tonnes per year. This compares well with the IPCC measurement evaluation of 32 million tonnes per year annual accumulation (Houghton *et al.* 1992) during the late 1980s and early 1990s. The close agreement in the annual rates of increase of the global methane inventories between observations and the model calculations is heartening and provides confidence that the model is providing an adequate description of the tropospheric OH oxidation sink. This can be confirmed by comparing the model and observed estimates (Houghton *et al.* 1992) of the methane lifetime, which are 10.95 and 11 years respectively.

The comparison of the model with observations for methane is most revealing for surface locations in the Southern Hemisphere because of remoteness from the major emissions. Figure 2 shows a comparison of the model results for 36–42° S with the observations of Fraser *et al.* (1986) and Steele *et al.* (1987) for Cape Grim 41° S and Amsterdam Island 39° S respectively. The model is providing a realistic and quantitative description of hydroxyl radical oxidation of methane. However, even at these remote southern latitudes, the influence of emission regions can still be discerned in the model results. Indeed, the assumed seasonal variations in the paddy field and biomass burning methane sources account for much of the calculated seasonal cycle.

(*b*) *Ozone*

Ozone is a key model constituent because of its importance as a radiatively active gas (Fishman *et al.* 1977) and because of its possible influence by human activities (Crutzen 1974). In the 10 year model experiments described here, annual global

PHILOSOPHICAL TRANSACTIONS OF THE ROYAL SOCIETY A MATHEMATICAL, PHYSICAL & ENGINEERING SCIENCES

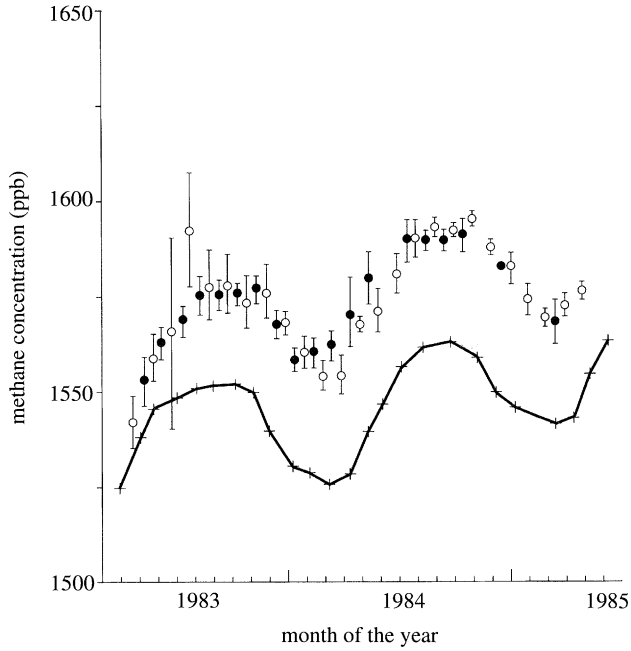

Figure 2. Comparison of the model results with surface observations for methane in the Southern Hemisphere.

tropospheric (up to 12 km altitude; pole-to-pole) photochemical production and destruction were approximately balanced at 5240 and 4600 million tonnes per year respectively. Transport from the stratosphere and dry deposition were significantly smaller in magnitude at 1080 and 1420 million tonnes per year. The global total tropospheric ozone destruction rate amounted to 5660 million tonnes per year, which when taken with the global tropospheric inventory of 350 million tonnes, gave a tropospheric lifetime of 23 days.

Almost every aspect of the model assumptions and input has some impact on model calculated ozone concentrations. Comparison of model against observations for ozone is therefore important component of an evaluation of model performance. Here, the electrochemical concentration cell (ECC) ozonesonde observations taken at nine stations provide a self-consistent ozone database (Komhyr *et al.* 1989) against which to compare model calculations. This comparison is illustrated in figure 3 for a selection of stations and seasons.

Best agreement was obtained for Boulder (40° N) and Hilo (19° N) stations in winter, where both the observed profile shape and absolute concentrations were reproduced by the model. Agreement at low latitudes was relatively poorer. For example, at Samoa (14° S), the model over estimates the ozonesondes by approaching a factor of three in the middle troposphere. Even the profile shape is not well reproduced, with the steepening in the concentration increase with altitude setting in several kilometers lower than is observed. Agreement is relatively good in the polar regions of both hemispheres in both altitude profile and absolute concentrations.

Surface ozone concentrations were relatively well described by the model, both in terms of the magnitudes of monthly average concentrations and in the shape of their diurnal cycles. These surface results have been reported previously (Hough &

PHILOSOPHICAL TRANSACTIONS OF THE ROYAL SOCIETY A MATHEMATICAL, PHYSICAL & ENGINEERING SCIENCES

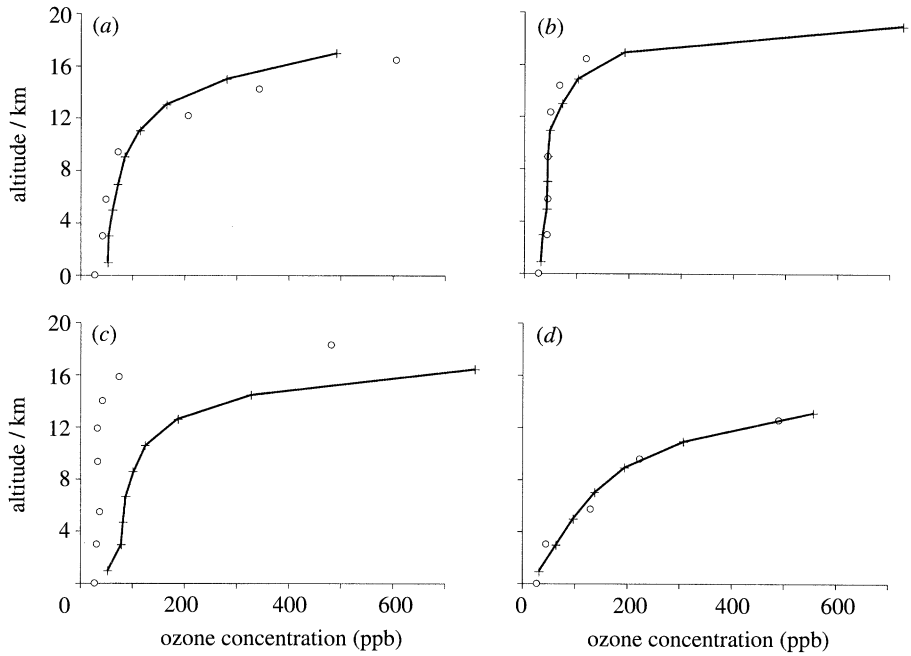

Figure 3. Comparison of the model results with ozonesonde measurements.

Derwent 1990; Hough 1991) and were not significantly influenced by the changes made to correct poor model performance for ozone in the lower stratosphere.

The ozone inventory, integrated from pole-to-pole and up to 24 km, showed a small, but steady annual increase of about 0.06% throughout the model experiment. This is consistent with reported increases in ozone throughout the troposphere during the 1980s over the continental regions of Europe (Staehelin *et al.* 1991), but with little evidence of any significant and consistent trends elsewhere.

(*c*) *Carbon monoxide*

The first IPCC report (Houghton *et al.* 1990), in reviewing the observational database for carbon monoxide, explains that because of its short lifetime, coupled with an inadequate monitoring network, global spatial variability and long term trends are not well-documented. The limited database demonstrates that:

CO concentrations about a factor of two higher in the Northern Hemisphere (100–120 ppb) compared with the Southern Hemisphere (50–60 ppb),

CO concentrations are increasing at about 1% per year in the Northern Hemisphere but there is little evidence for growth in the Southern Hemisphere.

In the two-dimensional model, oxidation of carbon monoxide by hydroxyl radicals in the troposphere accounts for the vast majority (94%) of the carbon monoxide, with dry deposition accounting for the small remainder. Direct emissions from human activities, including both motor vehicles and biomass burning, were almost equal in magnitude to that from hydrocarbon oxidation. The total tropospheric removal rate of 3120 million tonnes per year, when taken with the global inventory of 465 million tonnes, combines to give a turn-over time of 54 days.

Over the 10 year model calculation, sources and sinks for carbon monoxide did not stay in balance. Due to a slight preponderance of the former over the latter, the total

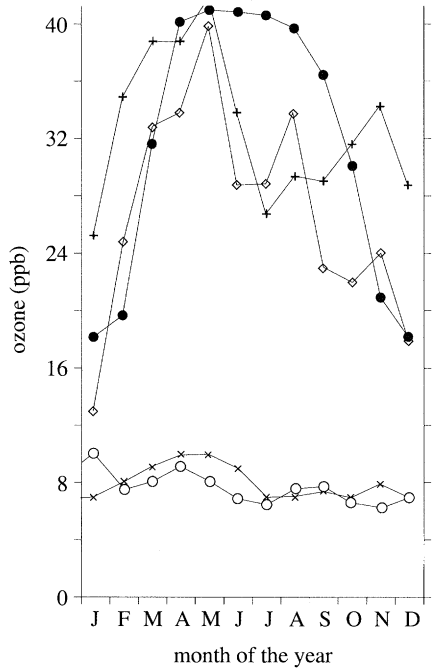

Figure 4. Comparison of the model results with surface ozone measurements.

global carbon monoxide inventory steadily increased. The annual increase, averaged over the last five years of the calculation, amounted to 0.25% per year. The model behaviour is consistent with the carbon monoxide trends as reviewed in Houghton *et al.* (1990).

As regards concentration distribution, the mean annual Northern and Southern Hemisphere surface concentrations in the model were found to be 95 and 195 ppb, respectively. Although the concentration ratio between the hemispheres agrees well with the observations, the observed surface concentrations (Houghton *et al.* 1990) are overestimated by about a factor of two. The apparent overestimation of surface carbon monoxide concentrations is illustrated in figure 5. Here, carbon monoxide measurements for Mace Head, Ireland are compared with model results, showing excellent agreement in the size and timing of the seasonal cycle and a factor of two overestimation of the observations.

The comparison of model with observations suggests that carbon monoxide emissions have been overestimated in the model by a large margin. That such overestimations can occur, despite reasonable predictions being returned for hydroxyl radical concentrations, has already been explained in the introductory paragraphs above. It arises because the hydroxyl radical concentrations are not particularly sensitive to the carbon monoxide concentrations and hence emissions. This is caused by the overriding importance of the OH + CO reaction and that its competing reaction OH + CH_4 is a major carbon monoxide source. Hence the lack of, or presence of, any agreement between model and observation for carbon monoxide does not constrain the mean tropospheric hydroxyl distribution, because of the uncertainty in the global carbon monoxide source strength. Attention is directed to the isotopic distribution in

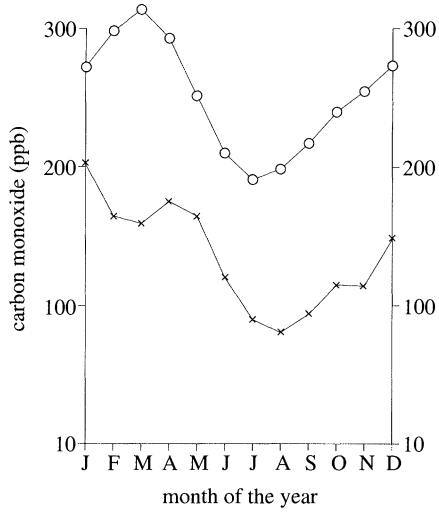

Figure 5. Comparison of the model results with surface carbon monoxide measurements.

atmospheric carbon monoxide in the next section of this study, to constrain further the carbon monoxide budget.

(*d*) *Carbon-14 monoxide*

The atmospheric carbon monoxide exists in several isotopic forms, one of which ^{14}CO has been useful in understanding the tropospheric distribution of hydroxyl radicals. Table 5 contains the details of the ^{14}CO sources which have been included in this two-dimensional model study. The main source, cosmic ray production, is moderately well quantified and is believed to be concentrated in the upper troposphere and lower stratosphere. It exhibits a maximum in high latitudes and is modulated by the sunspot cycle (Lingenfelter 1963). The remaining sources are much smaller in magnitude and are distributed quite differently in space from the cosmic ray source.

Figure 6 compares the model calculated ^{14}CO concentrations with the latitudinal distribution for the middle of January from Mak *et al.* (1992), the seasonal variations at Baring Head, 41° S, from Brenninkmeijer *et al.* (1992) and at 43°–51° N from Volz *et al.* (1981). The general level of agreement between the model results and the observations is good. The model appears to underestimate slightly the Southern Hemisphere levels observed in the latitudinal distribution by about 10–30%. Model concentrations at 36°–42° S during June to December appear to overestimate the Baring Head observations by 20–30%, whereas the model underestimates the original Northern Hemisphere observations by about 20–30%.

The agreement between the available ^{14}CO measurements and the two-dimensional model results provides some confirmation that the major elements of the life cycle of ^{14}CO have been described with some realism. On this basis, the distribution of hydroxyl radicals in the troposphere calculated here can be assigned a probable accuracy of ±30%.

It is worth commenting that the agreement between model and observation appears to be slightly better for ^{14}CO, where the discrepancies are within ±30%, than for ^{12}CO, where they are within a factor of two. The main uncertainty in the ^{12}CO budget is the biospheric source strength from isoprene and terpene photooxidation. Because

Table 5. *Model sources of* ^{14}CO

source	isotopic ratio $\times 10^{12}$ per molecule	annual source strength g ^{14}CO per year
cosmic rays[a]		10 860
carbon monoxide emissions	0.88	1480
methane oxidation	1.104	994
hydrocarbon oxidation		
ethane	1.19	34
propane	1.16	21
butanes	0.75	8
pentanes	0.56	4
hexanes	0.42	3
ethylene	1.14	51
propylene	1.09	28
acetylene	0.67	3
benzene	0.56	2
toluene	0.18	1
isoprene	1.50	363
total	13 852	

[a] 2.18×10^{26} molecules ^{14}CO per year (from Mak *et al.* 1992).

of the important cosmic ray ^{14}CO production, biogenic sources do not dominate the ^{14}CO budget to anything like the same extent as for ^{12}CO.

(*e*) *Methyl chloroform*

The dominant fate of the methyl chloroform (1,1,1-trichloroethane) emitted into the model was reaction with hydroxyl radicals in the troposphere. In the 10 year model calculation, a constant methyl chloroform emission of 0.6 million tonnes per year was assumed based on the estimated emissions for the second half of the 1980s (Midgely 1989). Sources and sinks did not, however, remain in balance, with sources dominating over sinks. The annual increase in the methyl chloroform inventory amounted to an accumulation of about 0.099 million tonnes per year. This compares closely with the annual increases observed by the ALE-GAGE network over the 1980–1983 period of 0.111–0.155 million tonnes per year (Tie *et al.* 1992).

The close agreement in the annual rates of increase in the global methyl chloroform inventory between observations and model calculations (see figure 7) is most heartening. It confirms the view that the model is providing a realistic and quantitative description of OH oxidation. From a mass balance over the 10 year model experiment, the two-dimensional model life-time for methyl chloroform is estimated to be 6.6 years. This compares closely with the literature lifetimes of 6.3 and 5.7 years, respectively, from Prinn *et al.* (1987) using the mass-balance method and Tie *et al.* (1992) using a chemistry-transport model, including a small, additional ocean sink term.

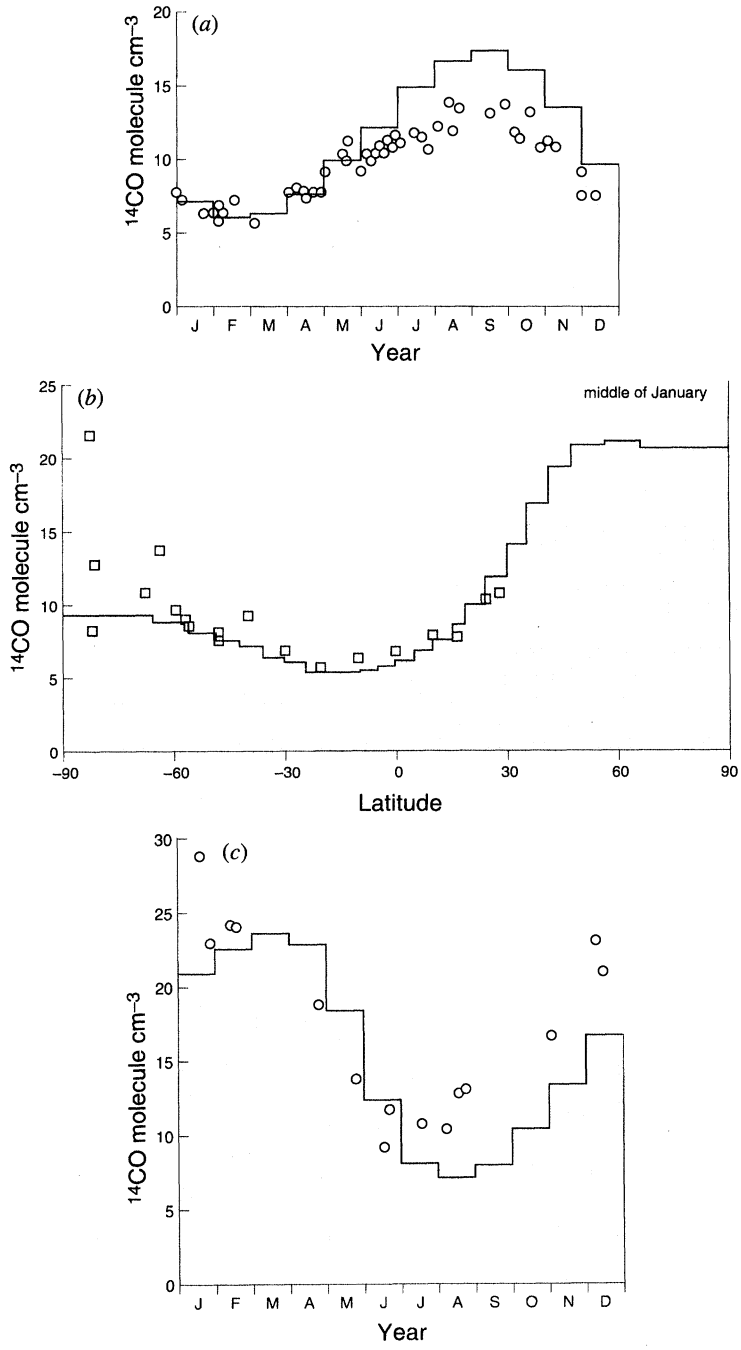

Figure 6. Comparison of the model results with surface ^{14}CO measurements.

(*f*) *Hydroxyl radicals*

The distribution of hydroxyl radicals in the two-dimensional model troposphere is controlled by the balance between free radical production and destruction, in each grid cell, during each day. The model uses 24-hour photolysis rate coefficients so

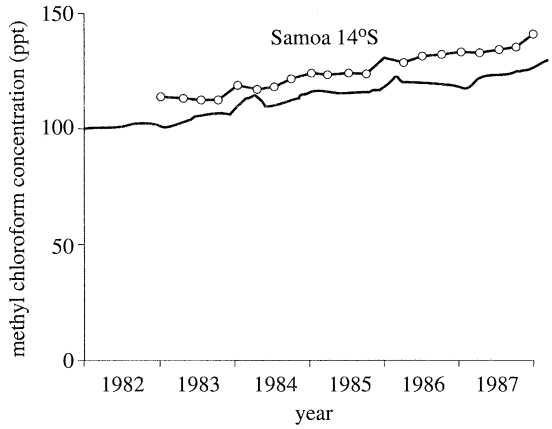

Figure 7. Comparison of the model results with surface methyl chloroform measurements.

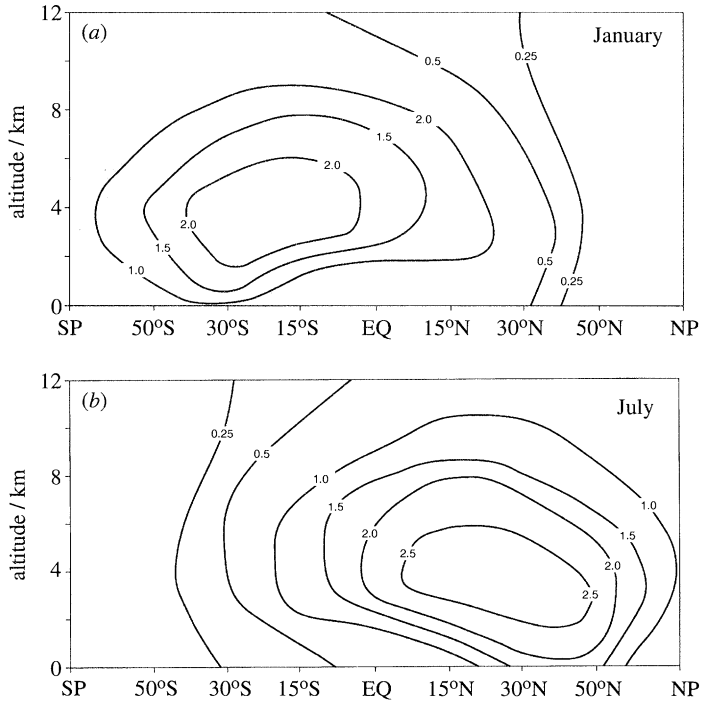

Figure 8. Latitude-altitude distributions of daily average hydroxyl radical concentrations for (*a*) mid-January and (*b*) mid-July.

the calculated hydroxyl radical concentrations should be accurate representations over the same averaging time period. Figure 8 *a*, *b* show the latitude-altitude 24-hour mean hydroxyl radical concentrations for mid-January and mid-July in the current troposphere.

Hydroxyl radical concentrations fall off towards high latitudes because of the influence of increasing solar zenith angles and total ozone column, partially compensated by increasing daylength in the respective Summer Hemisphere. It is not clear from

these figures whether the hemispheric mean hydroxyl radical concentrations are different, despite the great differences in trace gas emissions that they receive and the potentially different influence of human activities. In fact, the mean tropospheric hydroxyl radical concentrations in the winter hemispheres are not significantly different (Southern, July, 5.18×10^5 molecules cm^{-3}; Northern, January, 5.21×10^5 molecules cm^{-3}). However, the respective tropospheric mean hydroxyl radical concentrations in the summer hemispheres were different (Southern, January, 1.32×10^6; Northern, July, 1.67×10^6 molecules cm^{-3}). As will be demonstrated later, when a full treatment of the uncertainties in model concentrations is presented, the difference between the hemispheric means in summer is significant.

Over the years, there have been suggestions that the hemispheric mean concentrations differ significantly (Singh 1977). This work confirms that with the current evaluated chemical kinetics database and understanding of trace gas life cycles, two-dimensional chemical transport models indicate that interhemispheric differences in hydroxyl radical concentrations are probably important. The explanation is not that the Southern Hemisphere is remote from human influence, but that this influence is uneven between the hemispheres. This has much to do with the short lifetimes of NO_x and CO which result in much of Southern and Northern Hemispheres becoming ozone sinks and sources, respectively, under the influence of tropospheric photochemistry.

This study gives, as its best estimate for the mean, 0–12 km, pole-to-pole, tropospheric hydroxyl radical concentration in the current atmosphere, 1.01×10^6 molecules cm^{-3}. For the entire 0–24 km model domain the mean concentration decreases somewhat to 0.74×10^6 molecules cm^{-3}. These values are summarized in table 1.

(*g*) *Other organic compounds*

The hydroxyl radical oxidation sink for organic compounds is operating throughout the troposphere and determines the atmospheric lifetimes of the vast majority of compounds in this class. Lifetimes, together with emission rates, determine the global concentrations of each compound that would build up if emissions continued indefinitely. The atmospheric lifetimes of a large number of organic compounds emitted at the surface in the mid- and high-latitudes of the Northern Hemisphere are presented in table 6. These lifetimes have been estimated using the two-dimensional model developed in this study and evaluated chemical kinetic data covering rate coefficients for the reactions of hydroxyl radicals with organic compounds (Atkinson 1990).

4. Sensitivity to and uncertainty derived from chemical kinetics input data

(*a*) *Sensitivity of hydroxyl radical concentrations to chemical kinetics input data*

To examine the accuracy with which the free radical chemistry is represented in the two-dimensional model, the sensitivities of the output concentrations to the input rate coefficient values of 17 selected elementary reactions have been calculated. More strictly, a sensitivity parameter, a, has been defined as the change in the logarithm of the output concentration resulting from a small change in a particular rate coefficient divided by the change in the logarithm of the rate coefficient. The rate coefficient for each of the reaction to be studied was increased by a factor of d,

PHILOSOPHICAL TRANSACTIONS OF THE ROYAL SOCIETY A MATHEMATICAL, PHYSICAL & ENGINEERING SCIENCES

Table 6. *Atmospheric lifetimes*

(Lifetimes are calculated for a range of organic compounds for tropospheric OH oxidation using the global two-dimensional model and a review of tropospheric chemistry (Atkinson 1992).)

compound	lifetime/days	compound	lifetime/days
methane	3781	beta-pinene	0.4
ethane	116	3-carene	0.4
propane	27.0	limonene	0.2
n-butane	12.2	1,3-butadiene	0.5
2-methylpropane	13.3	isoprene	0.3
n-pentane	7.9	acetylene	34.5
2-methylbutane	8.0	methylacetylene	5.3
2,2-dimethylpropane	36.6	1-butyne	3.9
n-hexane	5.5	2-butyne	1.2
2-methylpentane	5.5	benzene	25.3
3-methylpentane	5.4	toluene	5.2
2,2-dimethylbutane	13.4	ethylbenzene	4.4
2,3-dimethylbutane	4.9	n-propylbenzene	5.2
n-heptane	4.3	i-propylbenzene	4.8
2,2-dimethylpentane	9.1	t-butylbenzene	6.8
2,4-dimethylpentane	6.1	o-xylene	2.3
2,2,3-trimethylbutane	7.3	m-xylene	1.3
n-octane	3.6	p-xylene	2.2
2,2,4-trimethylpentane	8.4	o-ethyltoluene	2.5
2,3,4-trimethylpentane	4.4	m-ethyltoluene	1.6
2,2,3,3-tetramethylbutane	28.8	p-ethyltoluene	2.6
n-nonane	3.0	1,2,3-trimethylbenzene	0.9
n-decane	2.7	1,2,4-trimethylbenzene	1.0
n-undecane	2.4	1,3,5-trimethylbenzene	0.5
n-dodecane	2.2	tetralin	0.9
n-tridecane	1.9	napthalene	1.4
n-tetradecane	1.6	1-methylnaphthalene	0.6
n-pentadecane	1.4	2-methylnaphthalene	0.6
n-hexadecane	1.2	2,3-dimethylnaphthalene	0.4
cyclopropane	444	formaldehyde	3.2
cyclobutane	25.9	acetaldehyde	2.0
cyclopentane	6.0	proprionaldehyde	1.6
cyclohexane	4.1	butyraldehyde	1.3
cycloheptane	2.5	i-butyraldehyde	1.2
methylcyclohexane	3.0	valeraldehyde	1.1
ethylene	3.6	i-valeraldehyde	1.1
propylene	1.2	pivaldehyde	1.2
1-butene	1.0	hydroxyacetaldehyde	3.1

PHILOSOPHICAL TRANSACTIONS OF THE ROYAL SOCIETY A MATHEMATICAL, PHYSICAL & ENGINEERING SCIENCES

Table 6. *Cont.*

compound	lifetime/days	compound	lifetime/days
1-pentene	1.0	acetone	137
3-methyl-1-butene	1.0	methylethylketone	27.0
1-hexene	0.8	methylpropylketone	6.3
3,3-dimethyl-1-butene	1.1	diethylketone	15.5
1-heptene	0.8	methylbutylketone	3.4
2-methylpropene	0.6	ethylpropylketone	4.5
2-methyl-1-butene	0.5	methyl i-butylketone	2.2
cis 2-butene	0.6	glyoxal	2.7
cis 2-pentene	0.5	methylglyoxal	1.8
trans 2-butene	0.5	biacetyl	131
trans 2-pentene	0.5	methanol	33.3
2-methyl-2-butene	0.5	ethanol	9.5
2,3-dimethyl-2-butene	0.3	1-propanol	5.8
cyclopentene	0.5	2-propanol	6.0
cyclohexene	0.5	1-butanol	3.7
cycloheptene	0.4	2-methyl-2-propanol	27.7
1-methylcyclohexene	0.3	dimethyl ether	10.4
alpha-pinene	0.6	diethyl ether	2.3
methyl t-butyl ether	11.0	2-hexyl nitrate	9.8
formic acid	69.0	3-hexyl nitrate	11.5
acetic acid	42.0	cyclohexyl nitrate	9.4
methyl hydrogen peroxide	5.6	2-methyl-2-pentyl nitrate	18.1
t-butyl hydrogen peroxide	10.4	3-methyl-2-pentyl nitrate	10.3
acrolein	1.6	3-heptyl nitrate	8.4
methacrolein	0.9	3-octyl nitrate	8.0
crotonaldehyde	0.9	peroxyacetylnitrate	282
methylvinylketone	1.7	methyl chloroform	2409
methyl nitrate	914	CH_2FCF_3	5293
ethyl nitrate	63.4	C_2H_4F	504
1-propyl nitrate	50.1	$C_2F_3HCl_2$	475
2-propyl nitrate	75.8	C_2F_4HCl	2077
1-butyl nitrate	17.5	C_2HF_5	11753
2-butyl nitrate	33.8	$C_2FH_2Cl_3$	3602
2-pentyl nitrate	16.8	$C_2F_2H_3Cl$	7607
3-pentyl nitrate	27.7	$C_2H_3F_3$	18323
2-methyl-3-butyl nitrate	18.1	carbon monoxide	54.7
2,2-dimethyl-1-propyl nitrate	36.5		

taken to be $\exp(0.025) = 1.0253$, and the difference in the logarithms of the output concentrations, C, determined by rerunning the model experiment. The sensitivity

coefficient a is calculated accordingly:

$$a = \frac{\ln C_{(kd)} - \ln C_{(k)}}{\ln(kd) - \ln k} = \frac{\ln[C_{(kd)}/C_{(k)}]}{\ln d}.$$

In these calculations, each of the 17 key reaction rate coefficients was changed at the start of the model calculation and the changed values were maintained constant all the way through the model experiment. This is the commonest and most natural sensitivity concept and caters for the case where the parameter value is uncertain to a greater or lesser degree. The disadvantage of this approach is that it necessarily associates the uncertainty in a rate coefficient with the pre-exponential or temperature-independent part of each rate coefficient. For some reactions, temperature dependences may be more uncertain than rate coefficient values at ambient temperatures. Nevertheless, temperature dependences turn out not to be of crucial importance for the 17 key, elementary processes highlighted in this study and the temperature-independent sensitivity method suffices.

Table 7 shows the sensitivity coefficients calculated for the tropospheric mean hydroxyl radical concentration calculated for each rate coefficient. The compilations of evaluated rate coefficient data (Atkinson *et al.* 1992) used to set up the chemistry in the two-dimensional model, also provide evaluated estimates of uncertainty ranges. For many processes, these subjective uncertainty ranges are necessarily fairly broad. It has therefore been assumed that each rate coefficient is normally distributed within its subjective uncertainty range. Furthermore it has been assumed that this subjective range specifically defines the 5–95% confidence limits surrounding each rate coefficient.

On this basis, tabulated in table 7 are the values of $d \ln k$ for each rate coefficient from the data compilations and values of b, estimated from $ad \ln k$. The b values provide a measure of the contribution to the uncertainty in the tropospheric mean hydroxyl radical concentration from the uncertainty in each of the 17 key elementary rate coefficients. The chemical reactions have been ordered in importance in table 7 by their respective b values.

Apparently, there are seven chemical reactions which contribute significantly to the uncertianty in the mean hydroxyl radical concentration as shown by the b values. These are, in order of decreasing importance:

$$\mathrm{OH + NO_2 + M = HNO_3 + M},$$
$$\mathrm{CH_3O_2 + HO_2 = CH_3OOH + O_2},$$
$$\mathrm{NO + O_3 = NO_2 + O_2},$$
$$\mathrm{HO_2 + NO = OH + NO_2},$$
$$\mathrm{OH + HO_2 = H_2O + O_2},$$
$$\mathrm{HO_2 + O_3 = OH + O_2 + O_2},$$
$$\mathrm{OH + O_3 = HO_2 + O_2}.$$

The uncertainty in the ozone concentrations appears to be dominated by the free radical processes which together form the fast photochemical balance. The only process which contributes significantly to this uncertainty and does not form part of that balance system is the $\mathrm{NO + O_3}$ reaction. This reaction forms part of the $\mathrm{NO–O_3–NO_2}$ photostationary state balance by which ozone production is driven through the peroxy radical chemistry:

$$\mathrm{RO_2 + NO = NO_2 + RO},$$

PHILOSOPHICAL TRANSACTIONS OF THE ROYAL SOCIETY A MATHEMATICAL, PHYSICAL & ENGINEERING SCIENCES

Table 7. *Sensitivity coefficients for the tropospheric mean hydroxyl radical concentration to each thermochemical rate coefficients and their contribution to uncertainty*

($d \ln k$ values in natural logarithms were obtained from Atkinson *et al.* (1992). Column *a* gives the sensitivity coefficient to the reaction rate coefficient. Column *b* gives the value $a d \ln k$, that is the contribution to the uncertainty from that particular rate coefficient.)

reaction	$d \ln k$	sensitivity coefficient *a*	uncertainty contribution *b*
$OH + NO_2 + M$	0.23	−0.42	−0.097
$CH_3O_2 + HO_2$	0.7	−0.11	−0.077
$NO + O_3$	0.18	−0.39	−0.072
$OH + HO_2$	0.23	−0.25	−0.058
$OH + O_3$	0.35	−0.14	−0.048
$OH + CH_3O_2H$	0.46	−0.084	−0.039
$OH + CH_4$	0.23	−0.14	−0.032
$HO_2 + HO_2 + M$	0.35	−0.084	−0.029
$OH + H_2O_2$	0.23	−0.11	−0.026
PAN + M	0.92	−0.03	−0.026
$OH + H_2$	0.23	−0.06	−0.013
OH + HCHO	0.23	−0.06	−0.013
$NO_2 + O_3$	0.14	−0.03	−0.004
OH + CO	0.23	0.06	0.013
$CH_3O_2 + NO$	0.23	0.08	0.019
$HO_2 + O_3$	0.46	0.11	0.051
$HO_2 + NO$	0.23	0.28	0.064

NO_2 + radiation = NO + O,
O + O_2 + M = O_3 + M.
Overall
$RO_2 + O_2 = RO + O_3$.

It is clear that a great many reactions contribute little to the uncertainty in hydroxyl radical concentrations calculated in the two-dimensional model. It is arguable, though, whether they should be removed from the chemical mechanism. Their inclusion may well be crucial for the accurate assessment of other aspects of tropospheric chemistry, other than hydroxyl radical formation and destruction.

(*b*) *Uncertainties in hydroxyl radical concentrations due to chemical kinetics input data*

Once the importance of the sensitivity of the calculated hydroxyl radical concentrations to the individual elementary rate coefficients has been established, the next step is to address the combined uncertainty due to the combined sensitivity of all the rate coefficients. The calculation of the uncertainty in the calculated hydroxyl radical concentrations must necessarily assume that each of the rate coefficients could vary within its sensitivity range, completely independently of the values of the other rate coefficients.

By using a simulation program (LOTUS 1-2-3 ADD IN @RISK), which used latin hypercube sampling and 100 iterations, an assessment of the uncertain distributions of the calculated hydroxyl radical concentrations was built up. The assumption was made that each rate coefficient value was normally distributed within the uncertainty range quoted in the literature (Atkinson *et al.* 1992). The frequency distribution calculated for the mean tropospheric hydroxyl radical concentration obtained by combining together the uncertainties due to all the rate coefficients was approximately normal in shape. The 5–95% confidence range for the mean tropospheric hydroxyl radical concentration extends from 5.9–9.0 $\times$ 10^5 molecules cm^{-3}. On this basis, the current uncertainties in the rate coefficients appear to limit the accuracy of the mean tropospheric hydroxyl radical concentration to within a factor of 1.5 over a 2 σ confidence interval.

If the uncertainty range in the mean tropospheric hydroxyl radical concentration calculated in two-dimensional models is to be narrowed significantly in the future, then specific attention will need to be given to narrowing the uncertainty ranges in the literature estimates of the rate coefficients of up to about seven key chemical reactions, as follows:

$NO_2 + OH + M = HNO_3 + M,$
$O_3 + NO = NO_2 + O_2,$
$NO + HO_2 = OH + NO_2,$
$O_3 + HO_2 = OH + O_2 + O_2,$
$OH + HO_2 = H_2O + O_2,$
$CH_3O_2 + HO_2 = CH_3O_2H + O_2,$
$OH + O_3 = HO_2 + O_2.$

(*c*) *Sensitivity of other trace gases to chemical kinetics input*

Using the same methodology, it has been possible to define the sensitivity coefficients to chemical kinetics data for the mean model (0–24 km altitude; pole-to-pole) concentrations of methane and carbon monoxide as well as for the surface concentrations of ozone at 30° N. By folding in the evaluated uncertainty ranges in the chemical kinetic data, the contributions, *b*, to the uncertainty in these model output values can be estimated for each uncertain rate coefficient parameter.

For the mean model methane concentrations, sensitivity coefficients are much smaller that for OH and the rate coefficients for six chemical reactions dominate the output uncertainty, as follows:

$OH + CH_4 = H_2O + CH_3,$
$OH + NO_2 + M = HNO_3 + M,$
$CH_3O_2 + HO_2 = CH_3O_2H + O_2,$
$HO_2 + NO = OH + NO_2,$
$NO + O_3 = NO_2 + O_2,$
$HO_2 + HO_2 + M = H_2O_2 + O_2 + M.$

It is worth noting that these above investitgations have taken into account the recent revisions in the evaluated chemical kinetic data for the OH + methane reactions (Vahjiani & Ravishankara 1992).

For the model mean carbon monoxide concentration, sensitivity coefficients are significantly greater than for methane. Five rate coefficients dominate uncertainty and that for the OH + CO reaction is by far the most important. Sensitivity coef-

PHILOSOPHICAL TRANSACTIONS OF THE ROYAL SOCIETY A MATHEMATICAL, PHYSICAL & ENGINEERING SCIENCES

ficients are particularly small for surface ozone at 30° N during mid-January. Three reactions dominate the uncertainty in the calculated ozone concentrations and each involves NO_x, as follows:

$$OH + NO_2 + M = HNO_3 + M,$$
$$NO + O_3 = NO_2 + O_2,$$
$$HO_2 + NO = NO_2 + OH.$$

These conclusions about the model methane, carbon monoxide, surface ozone and tropospheric hydroxyl radical concentrations demonstrate that the values of each of the model output variables are influenced in a different way by the uncertainties in different input rate coefficient parameters. Nevertheless, by applying the techniques of sensitivity and uncertainty analysis, it is possible to ascertain which rate coefficients most influence model uncertainty and which could usefully benefit from further study in the laboratory. Altogether 10 processes have been found to influence uncertainty, to a significant and discernible extent.

5. The influence of human activities on past and future hydroxyl radical concentrations

Two-dimensional model calculations described here confirm current understanding of how the oxidising capacity of the troposphere, as defined by the mean tropospheric hydroxyl radical concentration, is governed by the concentration distributions of methane, CO, ozone and NO_x.

Each of these concentration distributions has been substantially influenced by human activities. In this section, the mean tropospheric hydroxyl radical concentration for the pre-industrial atmosphere and for various years in the future are estimated.

Considering, first, the pre-industrial troposphere, then this can be described in the model by setting to zero the emissions of the main tropospheric trace gases where a substantial involvement from human activities can be discerned in table 3. On this basis, the model calculations for the pre-industrial troposphere included only the following sources: soils, lightning, vegetation, oceans, wetlands and wild animals.

The mean tropospheric hydroxyl radical concentration was estimated to be 0.83×10^6 molecules cm^{-3}, averaged over the lowest 0–24 km of the atmosphere, about 13% higher than the present day value. This is the extent of the likely decrease in the oxidizing capacity of the troposphere which has resulted from human activities up to the present day.

Few trace gas measurements are available from pre-industrial times through to the present day to verify if the two-dimensional model changes in OH are in anyway meaningful. Measurements were made, however, of surface ozone between 1867 and 1893 at the Montsouris Observatory, Paris (Volz & Kley 1988). These are compared with the corresponding model values in figure 4, showing that the agreement is quite acceptable. Because the two-dimensional model is able to account for much of the observed growth in surface tropospheric ozone concentrations, we can have some confidence in the model calulated decline in tropospheric hydroxyl radical concentrations since pre-industrial times.

Moving on to the future then, it is important to quantify the extent to which the tropospheric concentrations of the main radiatively active gases: methane and ozone, will continue to rise in concentration. Some of this rise will be controlled by the

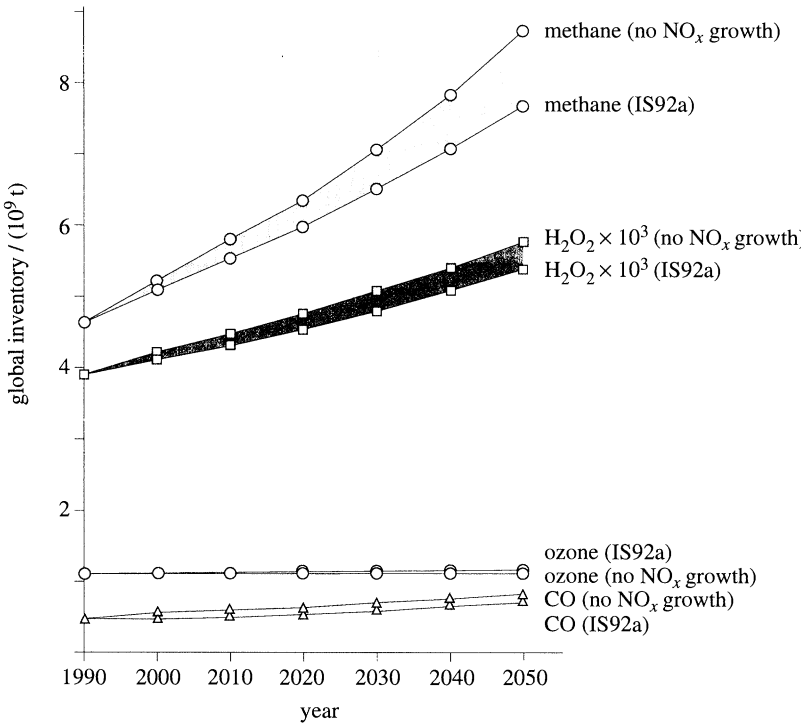

Figure 9. Total model inventories in million tonnes over the lowest 0–24 km for the period from 1990–2050 in the IS92a scenario.

future emissions of the major tropospheric source gases but the decreasing oxidising capacity of the troposphere will continue to play an important role in shaping future concentrations of those trace gases with OH-oxidation sinks. To illustrate the likely prospects for future methane and ozone concentrations, we need to be able to project the emissions of the major tropospheric trace gases into the future in some self-consistent manner. Emission projections are available for methane, CO, NO_x and volatile organic compounds (VOCs) (Houghton *et al.* 1992) and results for the main radiatively active gases are presented here for one 'business as usual' scenario, IS92a.

In response to the increasing emissions, the carbon monoxide, methane and NO_x concentrations increased steadily up to the year 2050. The overall impact of the growth in emissions was to reduce mean tropospheric hydroxyl radical concentrations by about 4.2% averaged over the lowest 0–24 km of the atmosphere over the period 1990–2050.

Figure 9 shows the growth in the global methane inventory in the IS92a scenario, amounting to an increase of 49% over the period 1990–2050. The trend in methane concentrations is considerably higher than expected on the basis of the increase in emissions alone, 30%, because of the changes in the tropospheric OH distribution which act to generate positive feedback on the methane growth. This positive feedback arises for two reasons. First, because increased methane concentrations shift the fast photochemical balance between OH and HO_2 radicals in favour of HO_2, allowing methane to build up even further. Second, because the increased methane levels bring increased carbon monoxide levels, which further shift the fast photochemical balance between OH and HO_2, leading again to increased methane levels.

The importance of the assumptions concerning future NO_x emissions in fixing the strength of the positive feedback in the future methane growth is also illustrated in figure 9. The alternative assumption of no future growth in NO_x emissions is studied as a sensitivity case to the central assumptions in the IS92a scenario case. The result is a substantial increase in the methane positive feedback, leading to a methane concentrations increases of about 60% between 1990 and 2050.

The corresponding changes in total model ozone inventories over the lowest 0–24 km of the atmosphere in figure 9 look small, corresponding to about an 8% increase over the period 1990–2050. However, the changes in ozone distribution are quite marked in the lower troposphere, relatively slight in the upper troposphere and so are somewhat disguised in the total ozone inventory statistics. Hydrogen peroxide, a major tropospheric oxidant, sees its model inventory increase quite dramatically in the IS92a scenario, see figure 9.

6. Discussion of the results

Understanding has grown over the years of the potential influence that human activities may have on the oxidising capacity of the troposphere. Undoubtedly, this understanding will need to underpin the efforts made by policy-makers to reduce emissions from human activities of certain tropospheric source gases. Currently coupled chemistry transport models offer the only way forward in assisting the formulation of policies which will protect and sustain this oxidizing capacity in the future. A stringent test of these models is their ability to represent the fast photochemical balance in the sunlit troposphere and hence produce a quantitative estimate of the concentration distribution of tropospheric hydroxyl radicals. A number of methods based on observations have been proposed to estimate the global mean hydroxyl radical concentration and hence to test the chemistry-transport models.

The life cycles of certain of the main tropospheric source gases rely on a balance between emission and hydroxyl radical destruction. It is therefore possible in principle to use observations and emissions to work back to the global mean hydroxyl radical concentration. For methane, carbon monoxide and hydrogen, the emissions are not well enough quantified to allow an accurate estimation to be made of the mean hydroxyl radical concentration. However, for two trace gases: methyl chloroform and ^{14}CO, emissions are well quantified and mean hydroxyl radical concentrations have been derived from observations (Derwent 1988).

The carbon-14 monoxide distribution has been used by Weinstock (1969) and by Volz *et al.* (1981) to estimate mean hydroxyl radical concentrations (see table 1). More recently, as discussed above, measurements of ^{14}CO have become available in the Southern Hemisphere. The model calculations show both underestimation and over estimation of the observations, in a way that cannot be fully resolved. The conclusion is that the calculated mean hydroxyl radical concentration is within $\pm 30\%$ of that required to support the observed field of ^{14}CO, but that it is difficult to narrow the uncertainty limits down further.

The two-dimenisonal model gives a reciprocal lifetime for methyl chloroform destruction due to hydroxyl radicals of 0.152 ± 0.04 per year, based on the uncertainties due to chemical kinetic input data alone. This estimate can be compared with the corresponding value based on the observed global methyl chloroform inventory from the ALE-GAGE observation network (Prinn *et al.* 1992) and the estimated release

to the atmosphere (Midgley 1989). Subtracting off reciprocal lifetime contributions from ocean uptake and stratospheric photolysis, the reciprocal lifetime due to OH-oxidation of methyl chloroform from the observations is 0.151 ± 0.025 per year, in excellent agreement with the two-dimensional model result.

With the accuracy of the currently available chemical kinetic data and of the representation of the many processes in chemistry-transport models, it appears that realistic estimates of the distribution of hydroxyl radicals in the troposphere can be constructed. Such models should be able to give a reasonable description of the likely future influence of human activities on the oxidizing capacity of the troposphere and its impact on policy development within the scope of the global climate change and stratospheric ozone layer depletion issues.

The help of Dr Colin Johnson, Harwell Laboratory with the chemical reaction flux analysis and with many useful discussions is gratefully appreciated. The support and encouragement of the Department of the Environment's Global Atmosphere Division is warmly appreciated.

References

Atkinson, R. 1990 Gas-phase tropospheric chemistry of organic compounds: a review. *Atmos. Environ.* **24**A, 1–41.

Atkinson, R., Baulch, D. L., Cox, R. A., Hampson, R. F., Kerr, J. A. & Troe, J. 1992 Evaluated kinetic and photochemical data for atmospheric chemistry. *J. Phys. Chem. Ref. Data* **21**, 1125–1568.

Barnett, J. J. & Corney, M. 1985 Middle atmosphere temperature reference model from satellite observations. *Adv. Space Res.* **5**, 125–134.

Bhartia, P. K., Klenk, K. F., Fleig, A. J., Wellemeyer, C. G. & Gordon, D. 1984 Intercomparison of Nimbus 7 solar backscattered ultraviolet ozone profiles with rocket, balloon and Umkehr profiles. *J. Geophys. Res.* **89**, 5227–5238.

Blake, D. R. & Rowland, F. S. 1986 World wide increase in tropospheric methane. *J. Atmos. Chem.* **4**, 43–62.

Brasseur, G., Hitchman, M. H., Walters, S., Dymek, M., Falise, E. & Pirre, M. 1990 An interactive chemical dynamical radiative two-dimensional model of the middle atmosphere. *J. Geophys. Res.* **95**, 5639–5655.

Brenninkmeijer, C. A. M., Manning, M. R., Lowe, D. C., Wallace, G., Sparks, R. J. & Volz-Thomas, A. 1992 Interhemispheric assymetry in OH abundance inferred from measurements of atmospheric ^{14}CO. *Nature, Lond.* **356**, 50–52.

Buriez, J. C., Bonnel, B., Fouquart, Y., Geleyn, J. F. & Morcrette, J. J. 1988 Comparison of model-generated and satellite-derived cloud cover and radiation budget. *J. Geophys. Res.* **93**, 3705–3719.

Butler, J., Elkins, J., Thompson, T., Hall, B., Swanson, T. & Koropalov, V. 1991 Oceanic consumption of CH_3CCl_3: implications for tropospheric OH. *J. Geophys. Res.* **96**, 22347–22355.

Chameides, W. L. & Tan, A. 1981 The two-dimensional diagnostic model for tropospheric OH: an uncertainty analysis. *J. Geophys. Res.* **96**, 22347–22355.

Chameides, W. L., Davis, D. D., Bradshaw, J., Rodgers, M., Sandholm, S. & Bai, D. B. 1987 An estimate of the NO_x production rate in electrified clouds based on NO observations from the GTE/CITE 1 fall 1983 operation. *J. Geophys. Res.* **92**, 2153–2156.

Chang, J. S., Wuebbles, D. J. & Davis, D. D. 1977 A theoroetical model of global tropospheric OH distributions. UCRL-78392 Report, Lawrence Livermore Laboratory, California, USA.

Cicerone, R. J. 1988 How has the atmospheric concentration of CO changed? In *The changing atmosphere* (ed. F. S. Rowland & I. S. A. Isaksen), pp. 49–61. New York: John Wiley.

Cox, R. A., Derwent, R. G., Eggleton, A. E. J. & Lovelock, J. E. 1976 Photochemical oxidation of halocarbons. *Atmos. Environ.* **10**, 305–308.

PHILOSOPHICAL TRANSACTIONS OF THE ROYAL SOCIETY A MATHEMATICAL, PHYSICAL & ENGINEERING SCIENCES

Crutzen, P. J. 1974 Photochemical reactions intiated by and influencing ozone in the unpolluted troposphere. *Tellus* **26**, 47–57.

Crutzen, P. J. & Fishman, J. 1977 Average concentrations of OH in the troposphere and the budgets of CH_4, CO, H_2 and CH_3CCl_3. *Geophys. Res. Lett.* **4**, 321–324.

Crutzen, P. J. & Gidel, L. T. 1983 A two-dimensional photochemical model of the atmosphere, 2, the tropospheric budgets of the anthropogenic chlorocarbons, CO, CH_4, CH_3Cl and the effect of various NO_x sources on tropospheric ozone. *J. Geophys. Res.* **88**, 6641–6661.

Curtis, A. R. 1987*a* Discretisation of the zonally-averaged transport equation for use in global atmsopheric pollution studies. *AERE-R12524*. London: H.M. Stationery Office.

Curtis, A. R. 1987*b* Accurate conservative discretisation of transport equations retaining diagonal dominance. *AERE-R12523*. London: H.M. Stationery Office.

Curtis, A. R. & Sweetenham, W. P. 1987 FACSIMILE/CHEKMAT users manual. *AERE-R12805*. London: H M Stationery Office.

Derwent, R. G. 1988 The tropospheric lifetimes of halocarbons and their reactions with OH radicals: an assessment based on the concentration of 14-CO. Scientific Assessment of Stratospheric Ozone: 1989. Volume II Appendix AFEAS Report, pp. 127–148. WMO Global Ozone Research and Monitoring Report No. 20. WMO, Geneva, Switzerland.

Derwent, R. G. & Curtis, A. R. 1977 Two-dimensional model studies of some trace gases and free radicals in the troposphere. *AERE-R8853*. London: HMSO.

Dignon, J. & Hameed, S. 1989 Global emissions of nitrogen and sulphur oxides from 1860 to 1980. *J. Air Pollution Control Ass.* **39**, 180–186.

Ehhalt, D. H. & Drummond, J. W. 1988 The tropospheric cycle of NO_x. In *Chemistry of the unpolluted and polluted troposphere* (ed. H. W. Georgii & W. Jaeschke), pp. 219–251. Massachussetts, USA: D. Reidel.

Fishman, J., Ramanathan. V., Crutzen, P. J. & Liu, S. C. 1979 Tropospheric ozone and climate. *Nature, Lond.* **282**, 818–820.

Fraser, P. J., Hyson, P., Rasmussen, R. A., Crawford, A. J. & Khalil, M. A. K. 1986 Methane, carbon monoxide and methyl chloroform in the Southern Hemisphere. *J. Atmos. Chem.* **4**, 3–42.

Hansen, J., Johnson, D., Lacis, A., Lebedeff, S., Lee, P., Rind, D. & Russell, G. 1990 Global climate chnages as forecast by Goddard Institute for Space Studies three-dimensional model. *J. Geophys. Res.* **93**, 957–966.

Hough, A. M. 1989 The development of a two-dimensional global tropospheric model 1. The model transport. *Atmos. Environ.* **23**, 1235–1261.

Hough, A. M. 1991 Development of a two-dimensional global tropospheric model: model chemistry. *J. Geophys. Res.* **96**, 7325–7362.

Hough, A. M. & Derwent, R. G. 1990 Changes in the global concentration of tropospheric ozone due to human activities. *Nature, Lond.* **344**, 645–650.

Houghton, J. T., Jenkins, G. J. & Ephraums, J. J. 1990 *Climate change: the IPCC scientific assessment*. Cambridge University Press.

Houghton, J. T., Callander, B. A. & Varney, S. K. 1992 *Climate change 1992: the supplementary report to the IPCC scientific assessment*. Cambridge University Press.

Hughes, N. A. & Henderson-Sellers, A. 1985 Global 3D-nephanalysis of total cloud amount: climatology for 1979. *J. Clim. Appl. Meteorol.* **23**, 724–751.

Isaksen, I. S. A. 1980 The tropospheric ozone budget and possible man-made effects. In *Proc. Quadrennial Ozone Symp.*, pp. 845–852. Boulder, U.S.A.: NCAR.

Isaksen, I. S. A. & Hov, O. 1987 Calculation of trends in the tropospheric concentration of O_3, OH, CO, CH_4 and NO_x. *Tellus* B**33**, 271–285.

Komhyr, W. D., Oltmans, S. J., Francois, P. R., Evans, W. F. J. & Matthews, W. A. 1989 The latitudinal distribution of ozone to 35 km altitude from ECC ozonesonde observations, 1985–1987. In *Ozone in the atmosphere* (ed. R. D. Bojkov & P. Fabian), pp. 147–150. USA: DEEPAK Publishing.

Kraft, M. & Perner, D. 1993 Measurement of troposheric OH by laser long-path absorption spectroscopy. In *Proc. EUROTRAC Symp. 92* (ed. P. M. Borrell), pp. 239. The Hague, Netherlands: SPB Academic Publishing.

PHILOSOPHICAL TRANSACTIONS OF THE ROYAL SOCIETY A MATHEMATICAL, PHYSICAL & ENGINEERING SCIENCES

Levy, H. 1971 Normal atmosphere: large radical and formaldehyde concentrations predicted. *Science* **173**, 141–143.

Lingenfelter, R. E. 1963 production of carbon 14 by cosmic ray neutrons. *Rev. Geophys.* **1**, 35–55.

Logan, J. A. 1983 Nitrogen oxides in the troposphere: Global and regional budgets. *J. Geophys. Res.* **88**, 10785–10807.

Logan, J. A. 1985 Tropospheric ozone, seasonal behaviour, trends and anthropogenic influence. *J. Geophys. Res.* **90**, 10463–10482.

Lovelock, J. E. 1974 Atmospheric halocarbons and stratospheric ozone. *Nature, Lond.* **252**, 292–294.

Lovelock, J. E. 1977 Methyl chloroform in the troposphere as an indicator of OH radical abundance. *Nature, Lond.* **267**, 32.

Mahlman, J. D., Levy, H. & Moxim, W. J. 1980 Three-dimensional tracer structure and behaviour as simulated in two ozone precursor experiments. *J. Atmos. Sci.* **37**, 655–685.

Mak, J. E., Brenninkmeijer, C. A. M. & Manning, M. R. 1992 Evidence for a missing carbon monoxide sink based on tropospheric measurements of ^{14}CO. *Geophys. Res. Lett.* **19**, 1467–1470.

Midgley, P. 1989 The production and release to the atmosphere of 1,1,1-trichloroethane (methyl chloroform). *Atmos. Environ.* **23**, 2663–2665.

Neely, W. B. & Plonka, J. H. 1978 Estimation of time-averaged hydroxyl radical concentration in the troposphere. *Environ. Sci. Technol.* **12**, 317–321.

Oort, A. H. 1983 Global atmospheric circulation statistics. NOAA Prof. Paper 14 . Princeton, U.S.A.: GFDL.

Plumb, A. & Mahlman, J. D. 1987 The zonally-averaged transport characterisitics of the GFDL general circulation/transport model. *J. Atmos. Sci.* **44**, 298–327.

Prinn, R., Cunnold, D., Simmonds, P., Alyea, F., Boldi, R., Crawford, A., Fraser, P., Gutzler, D., Hartley, D., Rosen, R. & Rasmussen, R. 1992 Global average concentration and trend for hydroxyl radicals deduced from ALE/GAGE trichloro-ethane (methyl chloroform) data for 1978–1990. *J. Geophys. Res.* **97**, 2445–2461.

Rasmussen, R. A. & Khalil, M. A. K. 1984 Atmospheric methane in the real and ancient atmospheres: concentrations and interhemispheric gradient. *J. Geophys. Res.* **89**, 11599–11605.

Singh, H. B. 1977*a* Atmospheric halocarbons: evidence in favor of reduced average hydroxyl radical concentrations in the troposphere. *Geophys. Res. Lett.* **4**, 101–104.

Singh, H. B. 1977*b* preliminary estimation of average tropspheric HO concentrations in the Northern and Southern Hemispheres. *Geophys. Res. Lett.* **4**, 453–456.

Staehelin, J. & Schmid, W. 1991 Trens analysis of tropospheric ozone concentrations utilising the 20-year data set of ozone balloon soundings over Payerne (Switzerland). *Atmos. Environ.* **25**A, 1739–1749.

Steele, L. P., Frazer, P. J., Rasmussen, R. A., Khalil, M. A. K., Conway, T. J., Crawford, A. J., Gammon, R. H., Masarie, K. A. & Thoning, K. W. 1987 The global distribution of methane in the troposphere. *J. Atmos. Chem.* **5**, 125–171.

Strand, A. & Hov, O. 1993 A two-dimensional zonally-averaged transport model including convective motions and a new strategy for the numerical solution. *J. Geophys. Res.* **98**, 9023–9037.

Talukdar, R., Mellouki, A., Schmoltner, A. M., Watson, T., Montzka, S. & Ravishankara, A. R. 1992 Kinetics of the OH reaction with methyl chloroform and its atmospheric implications. *Science* **257**, 227–230.

Taylor, J. A., Brasseur, G., Zimmerman, P. R. & Cicerone, R. J. 1991 A study of the sources and sinks of methane and methyl chloroform using a Lagrangian tropospheric tracer transport model. *J. Geophys. Res.* **96**, 3013–3044.

Thompson, A. M. & Cicerone, R. J. 1986 Possible perturbations to atmospheric CO, CH_4 and OH. *J. Geophys. Res.* **91**, 10853–10864.

Tie, X., Kao, C. Y., Mroz, E. J., Cicerone, R. J., Alyea, F. N. & Cunnold, D. M. 1992 Three-dimensional simulations of atmospheric methyl chloroform: effect of an ocean sink. *J. Geophys. Res.* **97**, 20751–20769.

PHILOSOPHICAL TRANSACTIONS OF THE ROYAL SOCIETY A MATHEMATICAL, PHYSICAL & ENGINEERING SCIENCES

Volz, A. & Kley, D. 1988 Evaluation of the Montsouris series of ozone measurements made in the nineteenth century. *Nature, Lond.* **332**, 240–242.

Volz, A., Ehhalt, D. H. & Derwent, R. G. 1981 Seasonal and latitudinal variation of ^{14}CO and the tropospheric concentration of OH radicals. *J. Geophys. Res.* **86**, 5163–5171.

Warneck, P. 1988 *Chemistry of the natural atmosphere*. San Diego, CA: Academic Press.

Warren, S. G., Hahn, C. J., London, J., Chervin, R. M. & Jenne, R. L. 1986 global distribution of total cloud cover and cloud type amounts over land. *Report NCAR/TN-273+STR*. Boulder, CO: NCAR.

Weinstock, B. 1969 The residence time of carbon monoxide in the atmosphere. *Science* **168**, 224–225.

WMO 1986 Atmospheric ozone 1985-Assessment of our understanding of the processes controlling its present distribution and change. Report 16. Geneva, Switzerland: World Meteorological Office.

WMO 1991 Scientific Assessment of ozone depletion: 1991. World Meteorological Organisation. Global ozone research and monitoring, report no. 25. Geneva, Switzerland.

Wuebbles, D. J., Tamaresis, J. S. & Patten, K. O. 1994 Quantified estimates of total GWPs for greenhouse gases taking into account tropospheric chemistry. Global Climate Research Division, Lawrence Livermore National Laboratory, Livermore, CA.

Received 2 March 1994; revised 7 March 1995; accepted 22 June 1995

PHILOSOPHICAL TRANSACTIONS OF THE ROYAL SOCIETY A MATHEMATICAL, PHYSICAL & ENGINEERING SCIENCES